



# Improved Diffuse Reflection Models for Computer Vision

LAWRENCE B. WOLFF

*Computer Vision Laboratory, Department of Computer Science, The Johns Hopkins University,  
Baltimore, MD 21218*

SHREE K. NAYAR

*Center for Research in Intelligent Systems, Department of Computer Science, Columbia University,  
New York, NY 10027*

MICHAEL OREN\*

*Artificial Intelligence Laboratory, Massachusetts Institute of Technology, Cambridge, MA 02139*

*Received December 18, 1996; Revised October 29, 1997; Accepted March 10, 1998*

**Abstract.** There are many computational vision techniques that fundamentally rely upon assumptions about the nature of diffuse reflection from object surfaces consisting of commonly occurring nonmetallic materials. Probably the most prevalent assumption made about diffuse reflection by computer vision researchers is that its reflected radiance distribution is described by the Lambertian model, whether the surface is rough or smooth. While computationally and mathematically a relatively simple model, in physical reality the Lambertian model is deficient in accurately describing the reflected radiance distribution for both rough and smooth nonmetallic surfaces. Recently, in computer vision diffuse reflectance models have been proposed separately for rough, and, smooth nonconducting dielectric surfaces each of these models accurately predicting salient non-Lambertian phenomena that have important bearing on computer vision methods relying upon assumptions about diffuse reflection. Together these reflectance models are complementary in their respective applicability to rough and smooth surfaces. A unified treatment is presented here detailing important deviations from Lambertian behavior for both rough and smooth surfaces. Some speculation is given as to how these separate diffuse reflectance models may be combined.

**Keywords:** reflectance and appearance rendering, shape-from-reflectance, shape-from-shading, physics-based vision

## 1. Introduction

In computer vision a widely used assumption about diffuse reflection from nonmetallic materials, is Lambert's law (Lambert, 1760), namely the expression:

$$\frac{1}{\pi} L_i \rho \cos \theta_i d\omega, \quad (1)$$

where radiance  $L_i$  is incident at angle  $\theta_i$  relative to the surface normal through solid angle  $d\omega$ , and where  $\rho$  is termed the *diffuse albedo* in the range [0, 1.0]. This reflectance model is typically instantiated into the implementation of a large number of algorithms such as shape-from-shading, photometric stereo (Horn and Brooks, 1989) and photometric-based binocular stereo (Grimson, 1984; Smith, 1986). It is therefore important for researchers in the computer vision community who utilize assumptions about diffuse reflection to be aware of the conditions under which there is significant

\*Current address: D.E. Shaw & Co., 39th Floor, 120 W. 45 Street, New York, NY 10036.

deviation from Lambert's law, and what other reflection models should be used.

It should be emphasized that the non-Lambertian diffuse reflection effects discussed here are separate from specular surface-air interface reflection phenomena such as discussed in (Torrance and Sparrow, 1967; Beckmann and Spizzichino, 1963; Nayar et al., 1991). Figure 1 illustrates this distinction more clearly. The top of Fig. 1 shows the typical three-lobes occurring for reflection of light from surfaces. Of the two surface reflectance lobes the "specular-spike" lobe is more dominant for smooth surfaces while the broader specular surface reflectance lobe becomes most dominant for high surface roughness. Figure 1(a) shows how light is specularly reflected from a smooth surface-air interface, where the term "smooth" implies that the standard deviation of height across the surface-air interface is orders of magnitude smaller than the wavelength of incident light. Specular reflection from dielectrics under these conditions is dictated by Fresnel theory (Fresnel, 1866; Siegal and Howell, 1981) which attenuates light

energy dependent upon the simple index of refraction  $n$  for the dielectric and the angle of incidence relative to the surface normal  $\theta_i$ . The attenuation factor,  $0 \leq F(\theta_i, n) \leq 1.0$ , is given by

$$F(\theta_i, n) = \frac{1}{2} \frac{\sin^2(\theta_i - \theta_t)}{\sin^2(\theta_i + \theta_t)} \left[ 1 + \frac{\cos^2(\theta_i + \theta_t)}{\cos^2(\theta_i - \theta_t)} \right], \quad (2)$$

where the transmission angle  $\theta_t$  of light into the dielectric is given by Snell's law:

$$\frac{\sin \theta_i}{\sin \theta_t} = n \rightarrow \theta_t = \sin^{-1} \left( \frac{\sin \theta_i}{n} \right).$$

The Torrance-Sparrow specular reflection model (Torrance and Sparrow, 1967) assumes that rough surfaces locally consist of an orientation distribution of smooth microfacet surfaces for which Fresnel theory individually applies to each microfacet. Specular reflection from a rough surface is the collective specular reflection from the variously oriented microfacets

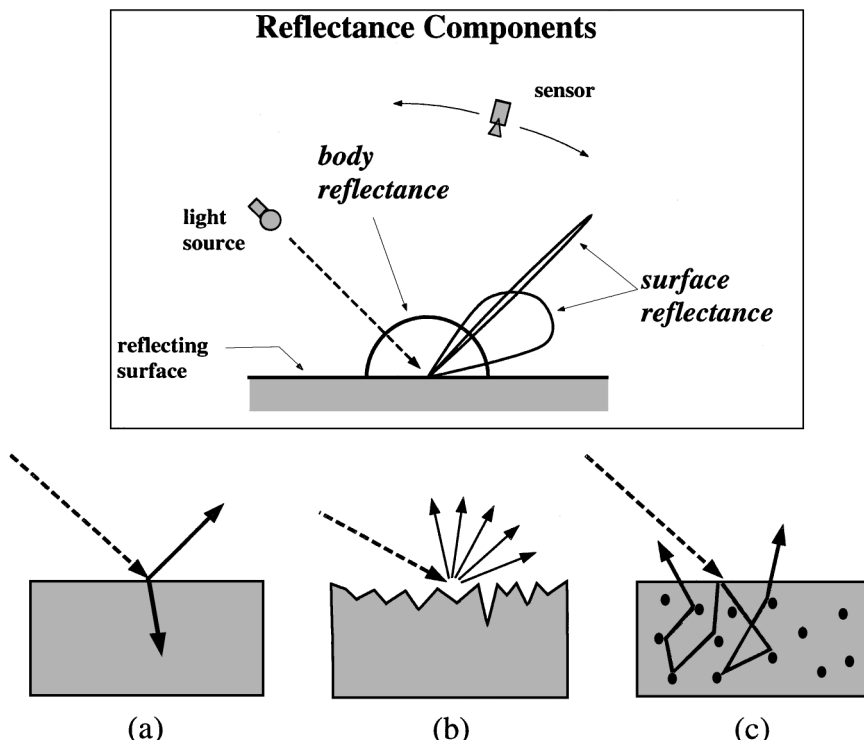


Figure 1. (Top) Polar plots of the different reflectance components. The plots show the intensity of the reflected light as a function of the viewer direction. Here, the body reflectance is assumed to be Lambertian. (a) Interface between two media with different refractive indices, (b) effect of the interface roughness, and (c) subsurface scattering.

(Fig. 1(b)) producing a broader specular reflectance lobe. Key to accurate empirical prediction of the Torrance-Sparrow model is the V-groove geometric analysis of how microfacets shadow and mutually mask specular reflection. Although specular reflection from a rough surface can be broad in many directions, this is still a phenomenon that only involves the surface-air interface and is *not* considered to be diffuse reflection as is sometimes confused in the computer vision community.

Diffuse reflection is considered to arise from light that has penetrated the surface-air interface and through physical processes that include scattering and refraction re-emerge into air as depicted in Fig. 1(c). Since light becomes exponentially attenuated in media with significant electrical conductivity, very little to virtually no diffuse reflection occurs from metals which is why diffuse reflection models are only applicable to dielectrics. The polar plot of the diffuse body reflectance lobe at the top of Fig. 1 depicting equal reflection in all directions consistent with Lambert's law is meant only as an illustration to distinguish diffuse reflection from surface-air interface reflectance phenomena.

Recently, two diffuse reflectance models have been separately derived from first principles by computer vision researchers each producing a considerable improvement over the Lambertian model for different surface conditions. The model proposed by Oren and Nayar (1995) shows that under very rough surface conditions geometric effects are so dominant that diffuse reflection from an individual smooth microfacet as depicted in Fig. 1(c) can be *approximated* to be Lambertian and yet collectively the combination of such reflection from all microfacets produces accurate diffuse reflection from the rough surface. This is not to imply that diffuse reflection from smooth surfaces by themselves are Lambertian. The model proposed by Wolff (1994a) shows that physical modeling of subsurface optical scattering phenomena in combination with surface optical boundary conditions is essential for determining the diffuse reflection characteristics of smooth and mildly rough dielectric surfaces. In general, this must be taken into account when geometric effects of the surface do not dominate.

A number of papers from the applied physics and optics community have studied reflectance and transmission of light from diffuse scattering within dielectric media (Kubelka and Munk, 1931; Orchard, 1969; Reichman, 1973; Bahar, 1987). Some of these papers have presented theories for both reflectance and

transmission for arbitrary optical thicknesses of scattering media, using collimated or diffuse light sources. In relation to the optics literature, the Wolff model (Wolff, 1994a) studies the specific case of diffuse reflectance from a semi-infinite, plane-parallel, inhomogeneous dielectric, which is most relevant to diffuse reflection observed in computer vision and computer graphics. In computer vision Healey (1989) has used the Kubelka-Munk model (Kubelka and Munk, 1931) to perform color insensitive segmentation. In computer graphics Hanrahan and Krueger (1993) used a subsurface scattering model to render the appearance of flat opaque and translucent objects.

The topic of rough diffuse surfaces has been extensively studied in the areas of applied physics and geophysics. In 1924, Opik designed an empirical model to describe the non-Lambertian behavior of the moon (Opik, 1924). In 1941, Minnaert modified Opik's model to obtain the following reflectance function (Minnaert, 1941):

$$f_r = \frac{k+1}{2\pi} (\cos \theta_i \cos \theta_r)^{(k-1)} \quad (0 \leq k \leq 1)$$

where,  $\theta_i$  and  $\theta_r$  are the polar angles of incidence and reflection, and  $k$  is a measure of surface roughness. This function was designed to obey Helmholtz's reciprocity principle (see Beckmann and Spizzichino, 1963) but is not based on any theoretical foundation. It assumes that the radiance of non-Lambertian diffuse surfaces is symmetrical with respect to the surface normal, an assumption that proves to be incorrect. Hapke and van Horn (1963) also obtained reflectance measurements from rough diffuse surfaces by varying the source direction for a fixed sensor direction. They found the peak of the radiance function to be shifted from the peak position expected for a Lambertian surface. This was interpreted as a minor discrepancy and the Lambertian model was assumed to be a reasonable approximation. Measurements by Oren and Nayar (1995) show that non-Lambertian behavior is clearly noticeable and significant when viewer direction is varied rather than source direction. The studies for rough surfaces mentioned so far were attempts to design reflectance models based on measured reflectance data. In contrast, several investigators developed theoretical models for diffuse reflection from rough surfaces. These efforts were motivated primarily by the reflectance characteristics of the moon. Infrared emission and visible light reflection from the moon (see Orlova, 1956; Siegal and Howell, 1981) indicate that the moon's surface

radiates more energy back in the direction of the source (the sun) than in the normal direction or in the forward direction. This phenomenon is referred to as *backscattering*.<sup>1</sup> Smith (1967) modeled the roughness of the moon as a random process and assumed each point on the surface to be Lambertian in reflectance. Smith's analysis, however, was confined to the plane of incidence and is not easily extensible to reflections outside this plane. Further, Smith's model does not account for interreflection effects. Buhl et al. (1968) modeled the surface as a collection of spherical cavities. They analyzed interreflections using this surface geometry, but did not present a complete reflectance model that accounts for masking and shadowing effects for arbitrary angles of reflection and incidence. Subsequently, Hering and Smith (1970) derived a detailed thermal emission model for surfaces modeled as a collection of V-cavities. However, all the cavities are assumed to be identical and aligned in the same direction, namely, perpendicular to the source-viewer plane. This model is also limited to reflections in the plane of incidence. Recently, in computer graphics, Poulin and Fournier (1990) derived a diffuse reflectance function for anisotropic surfaces modeled as a collection of parallel cylindrical sections. However, this result cannot be applied to surfaces with isotropic roughness. Other researchers in graphics have numerically pre-computed fairly complex reflectance functions and stored the results in the form of look-up tables or coefficients of spherical harmonic expansion (for examples, see Cabral et al., 1987; Kajiya, 1991; Westin et al., 1992; Gondek et al., 1994). This approach, though practical in many instances, does not replace the need for accurate analytical reflectance models.

Of importance to computer vision researchers, this paper gives a unified treatment in comparing improved diffuse reflectance models for rough surfaces (Oren-Nayar), and, smooth and mildly rough surfaces (Wolff) in a form that has direct bearing on computer

vision. The predicted radiance distributions for diffuse reflection according to these models are complete with respect to all possible illuminating source and viewer geometries. It is seen that significant deviation from Lambert's Law is prevalent for a number of physical conditions for both rough and smooth dielectric surfaces. Limitations of each of these diffuse reflectance models are described. In particular, it is shown at approximately what level of roughness each of these reflectance models is applicable. Further improvements towards a unified diffuse reflectance model for all cases of surface roughness are suggested.

## 2. Diffuse Reflection Models

Figure 2 defines notation for parameters used in the diffuse reflectance models described below. In this figure,  $\theta_i, \phi_i$  denotes incidence angle and incident azimuth angle respectively, and,  $\theta_r, \phi_r$  denotes reflected angle and reflected azimuth angle respectively. The expressions for diffuse reflection are in terms of reflected radiance  $L_r$  relative to incident radiance  $L_i$ . Formally, *radiance* is defined in the National Bureau of Standards monograph 160 (Nicodemus et al., 1977) as flux (Watts) per unit projected area ( $\cos \theta \cdot \text{meter}^2$ ) per unit solid angle (steradian); incident or reflected radiance expresses the flux of light per unit solid angle in a specified direction, respectively incident on or reflected from a unit foreshortened surface area.

### 2.1. Improved Diffuse Model for Rough Surfaces

The diffuse reflection model proposed by Oren and Nayar models the local geometry of rough surfaces as microfacets arranged in V-grooves, these microfacets distributed over various orientations (Oren and Nayar, 1992, 1993a, 1993b, 1994, 1995; Nayar and Oren, 1995). For tractability of the analysis of geometrical

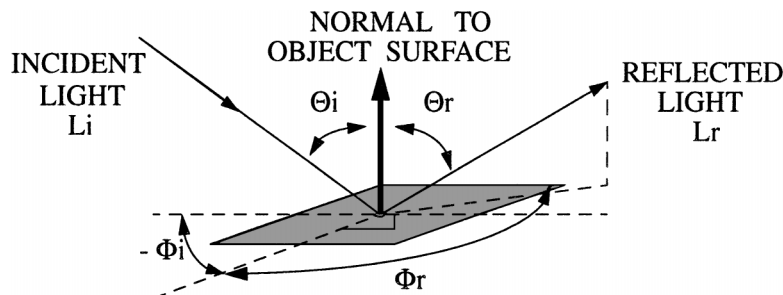


Figure 2. Definition of diffuse reflection parameters.

effects, the diffuse reflectance of each micro-facet is approximated to be Lambertian. The true nature of diffuse reflection from rough surfaces arises from combined reflection from these Lambertian microfacets subject to masking, shadowing and even interreflection effects. For a Gaussian Slope-Area distribution of microfacet orientations, the reflected radiance expressions derived for combined reflection from microfacets accounting for masking and shadowing are:

$$\begin{aligned} L_r^1(\theta_r, \theta_i, \phi_r - \phi_i; \sigma) &= \frac{\rho}{\pi} L_i \cos \theta_i \left[ C_1(\sigma) \right. \\ &\quad + \cos(\phi_r - \phi_i) C_2(\alpha; \beta; \phi_r - \phi_i; \sigma) \tan \beta \\ &\quad \left. + (1 - |\cos(\phi_r - \phi_i)|) C_3(\alpha; \beta; \sigma) \tan \left( \frac{\alpha + \beta}{2} \right) \right] \end{aligned} \quad (3)$$

where

$$\begin{aligned} C_1 &= 1 - 0.5 \frac{\sigma^2}{\sigma^2 + 0.33} \\ C_2 &= \begin{cases} 0.45 \frac{\sigma^2}{\sigma^2 + 0.09} \sin \alpha & \text{if } \cos(\phi_r - \phi_i) \geq 0 \\ 0.45 \frac{\sigma^2}{\sigma^2 + 0.09} \left( \sin \alpha - \left( \frac{2\beta}{\pi} \right)^3 \right) & \text{otherwise} \end{cases} \\ C_3 &= 0.125 \left( \frac{\sigma^2}{\sigma^2 + 0.09} \right) \left( \frac{4\alpha\beta}{\pi^2} \right)^2 \end{aligned}$$

$\sigma$  is the standard deviation of the Gaussian distribution as a measure of surface roughness,  $\alpha = \text{Max}[\theta_r, \theta_i]$ ,  $\beta = \text{Min}[\theta_r, \theta_i]$  and  $\rho$  is the diffuse albedo as defined for Lambert's Law.

The expression for reflected radiance from interreflection is derived to be

$$\begin{aligned} L_r^2(\theta_r, \theta_i, \phi_r - \phi_i; \sigma) &= 0.17 \frac{\rho^2}{\pi} L_i \cos \theta_i \frac{\sigma^2}{\sigma^2 + 0.13} \\ &\quad \times \left[ 1 - \cos(\phi_r - \phi_i) \left( \frac{2\beta}{\pi} \right)^2 \right] \end{aligned} \quad (4)$$

and the total reflected radiance resulting from all effects is:

$$\begin{aligned} L_r(\theta_r, \theta_i, \phi_r - \phi_i; \sigma) &= L_r^1(\theta_r, \theta_i, \phi_r - \phi_i; \sigma) + L_r^2(\theta_r, \theta_i, \phi_r - \phi_i; \sigma) \end{aligned} \quad (5)$$

Oren and Nayar propose a simplified expression for reflection from rough surfaces based upon the term  $C_3$  making a relatively small contribution and ignoring interreflections:

$$\begin{aligned} L_r^1(\theta_r, \theta_i, \phi_r - \phi_i; \sigma) &= \frac{\rho}{\pi} L_i \cos \theta_i (A + B \text{Max}[0, \cos(\phi_r - \phi_i)]) \\ &\quad \times \sin \alpha \tan \beta \end{aligned} \quad (6)$$

where

$$\begin{aligned} A &= 1 - 0.5 \frac{\sigma^2}{\sigma^2 + 0.33} \\ B &= 0.45 \frac{\sigma^2}{\sigma^2 + 0.09} \end{aligned}$$

This simplified expression has the advantage of being easier to incorporate into computer vision methods and is computationally efficient for graphics rendering.

An important consequence of the work of Oren and Nayar is that for very rough surfaces, the dominant factors that determine radiance are the geometrical effects caused by surface roughness and not the precise local diffuse reflectance characteristics. The approximation that was used for local diffuse reflectance, the Lambertian model, was sufficient to obtain a model that fits experimental data well. However, when the surface is relatively smooth, the geometrical effects are negligible and the exact model of local diffuse reflectance plays a critical role. This problem, of accurate modeling of local diffuse reflectance from smooth surfaces was studied by Wolff.

## 2.2. Improved Diffuse Model for Smooth Surfaces

The diffuse reflection model proposed by Wolff (1991, 1992a, 1992b, 1993a, 1993b, 1994a) models reflection from smooth dielectric materials as a combination of a subsurface light scattering distribution produced from internal inhomogeneities coupled with the refraction of externally incident and internally scattered light at the air-surface dielectric boundary. The following expression is derived for the radiance of diffuse surface reflection under the fundamental assumption that individual subsurface inhomogeneities isotropically scatter light:

$$\begin{aligned} \varrho L_i \times (1 - F(\theta_i, n)) \times \cos \theta_i \\ \times \left( 1 - F \left( \sin^{-1} \left( \frac{\sin \theta_r}{n} \right), 1/n \right) \right) d\omega \end{aligned} \quad (7)$$

The terms  $F(\cdot, \cdot)$  refer to the Fresnel reflection function (Siegal and Howell, 1981) shown in Eq. (2), and  $n$  is the index of refraction of the dielectric medium. Expression (7) deviates from the Lambertian term  $\cos \theta_i$  when the Fresnel reflection terms become significant.

The Fresnel function  $F(x, n)$  is a complicated algebraic expression in terms of  $x$  and  $n$ . Because almost all common dielectric materials have index of refraction,  $n$  in the range from 1.5 to 2.0, the Fresnel reflection function is weakly dependent upon this physical parameter over a wide range of dielectrics. The values of the Fresnel function can be stored in a small look-up table as a function of variable  $x$ , or, alternatively can be well approximated by the polynomial

$$F(x, n) = \frac{\left(\frac{2}{\pi}x\right)^5 + \epsilon}{1 + \epsilon}$$

where  $x$  is expressed in radians, and the value assigned to  $\epsilon$  is dependent upon the index of refraction  $n$ . The value for  $\epsilon$  is typically 0.07 for most dielectric materials. This simplification also makes it easier to incorporate into computer vision methods and is computationally efficient for graphics rendering.

A key feature of the diffuse reflection model proposed by Wolff is not only that it predicts the reflected radiance distribution in terms of  $\theta_i$  and  $\theta_r$ , but that it also precisely predicts the scaling factor  $\varrho$  for this distribution directly in terms of physical parameters intrinsic to the dielectric surface such as the index of refraction  $n$  and the *single scattering albedo* describing the proportion of energy  $0 \leq \rho \leq 1$  reradiated upon each subsurface single scattering. This scaling factor has the same role as the surface albedo for Lambert's Law except that it is completely physically motivated. The importance of the precise computation of  $\varrho$  to computer vision researchers lies in predicting the relative strength of specular and diffuse reflection as explained in detail in (Wolff, 1994b). While the expression for  $\varrho$  is complex, it can be treated independent of  $\theta_i$  and  $\theta_r$  in expression (7).

The expression for  $\varrho$  can be expressed as follows:

$$\varrho = \frac{\varrho_1}{1 - K} \quad (8)$$

where

$$\varrho_1 = \frac{\rho}{4\pi n^2} \frac{H_\rho(\bar{\mu}_{\text{inc}})H_\rho(\bar{\mu}_{\text{ref}})}{\bar{\mu}_{\text{inc}} + \bar{\mu}_{\text{ref}}},$$

$$\begin{aligned} \bar{\mu}_{\text{inc}} &= \sqrt{1 - \frac{\sin^2 \theta_i}{n^2}}, & \bar{\mu}_{\text{ref}} &= \sqrt{1 - \frac{\sin^2 \theta_r}{n^2}} \\ K &= \int_0^{\pi/2} F(\phi', 1/n) C_\rho \left( \cos \phi', \sqrt{1 - \frac{\sin^2 \theta_r}{n^2}} \right) \\ &\quad \times 2\pi \sin \phi' d\phi', \end{aligned}$$

and the function  $C_\rho(x, y)$  of incident and reflected angle variables,  $x$  and  $y$ , respectively defined by

$$C_\rho(x, y) = \frac{\rho}{4\pi} L \frac{x}{x + y} H_\rho(x) H_\rho(y),$$

An  $N$ th order approximation to the Chandrasekhar H-function (Chandrasekhar, 1960) can be expressed;

$$H_\rho(\mu) = \frac{1}{\mu_1, \dots, \mu_n} \frac{\prod_{i=1}^N (\mu + \mu_i)}{\prod_{\alpha} (1 + \kappa_{\alpha} \mu)},$$

defined in terms of the positive zeros  $\mu_i$  of the even Legendre polynomial of order  $2N$ , and the positive roots  $\kappa_{\alpha}$  of the associated *characteristic equation*;

$$1 = \sum_{j=1}^N \frac{a_j \rho}{1 - \kappa^2 \mu_j^2}.$$

### 3. Comparison of Diffuse Reflection Models for Rough and Smooth Surfaces

#### 3.1. Comparison of the Behavior of Reflected Radiance

A key characteristic of Lambert's Law (Eq. (1)) is that diffuse reflection is only dependent upon the angle of incidence of illumination  $\theta_i$  and therefore is independent of reflectance angle  $\theta_r$ , as well as azimuthal parameters  $\phi_i$  and  $\phi_r$ . From immediate observation of the reflected radiance distributions for Eqs. (3), (5), and (7), it is noted that diffuse reflection is in fact very much dependent upon reflectance angle for *both* rough and smooth surfaces. Figure 3 shows an example of dependence upon reflectance angle for a rough surface, in this case painted sandpaper, for various angles of incidence  $\theta_i$ . Figure 4 shows the dependence upon reflectance angle for a smooth surface of white Magnesium Oxide for normal incidence (i.e.,  $\theta_i = 0$ ).

For a given fixed angle of incidence, smooth surfaces have maximum reflected radiance at  $\theta_r = 0$  which is monotonic decreasing for increasing magnitude of  $\theta_r$

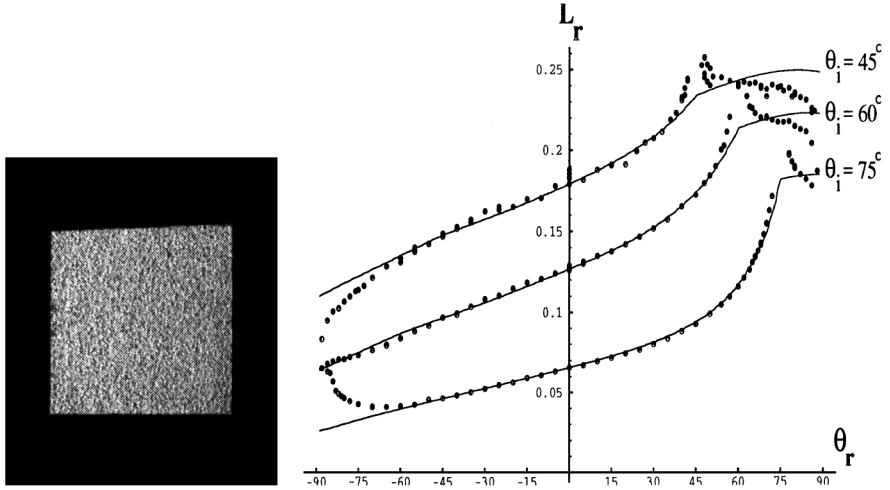


Figure 3. Diffuse reflection from a rough painted sandpaper surface ( $\sigma = 40^\circ$ ) as a Function of emittance angle  $\theta_r$  for various incidence angles  $\theta_i$ . Solid lines are predictions by the Oren-Nayar model.

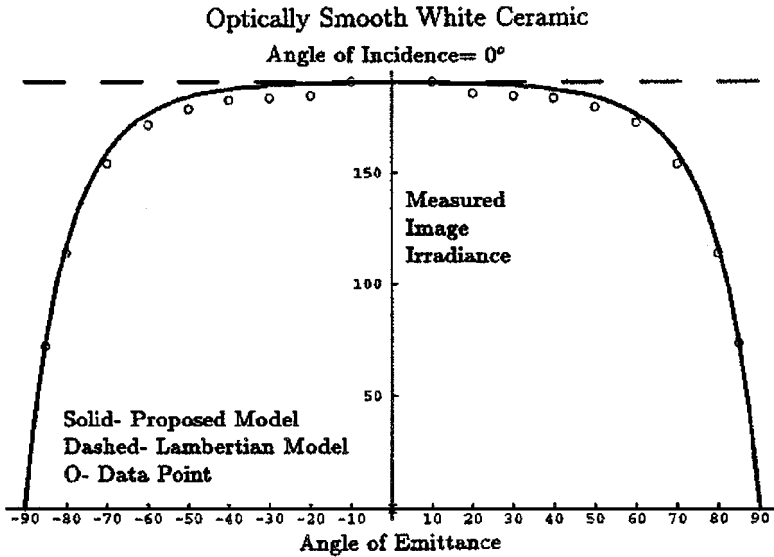


Figure 4. Diffuse reflection from a smooth white magnesium oxide surface, as a Function of emittance angle  $\theta_r$ , for normal incidence ( $\theta_i = 0$ ). Solid line is prediction by the Wolff model.

as shown in Fig. 3. The reflected radiance is symmetric about  $\theta_r = 0$  for smooth surfaces and is azimuth independent. For a given fixed angle of incidence the behavior of the dependence of diffuse reflected radiance from rough surfaces on reflected angle  $\theta_r$  is much more complicated. Furthermore, for rough surfaces Eqs. (3) and (5) show that diffuse reflection has additional dependence upon azimuthal geometry,  $\phi_i$  and  $\phi_r$ . As seen in the example of Fig. 3, reflected radiance can both increase or decrease as a function of increasing magnitude of  $\theta_r$ . As Oren and Nayar have pointed out,

the reflected radiance for rough surfaces is asymmetric about  $\theta_r = 0$  both in the plane of incidence<sup>2</sup> and outside the plane of incidence. Particularly for reflection directions contained in the plane of incidence, reflected radiance actually *increases* for increasing magnitude of  $\theta_r$  on the same side of the surface normal as an incident point light source, while *decreasing* for increasing magnitude of  $\theta_r$  on the opposite side of the surface normal from the light source.

Figure 5 shows the prediction by the Wolff model under the same illumination-viewing conditions as in

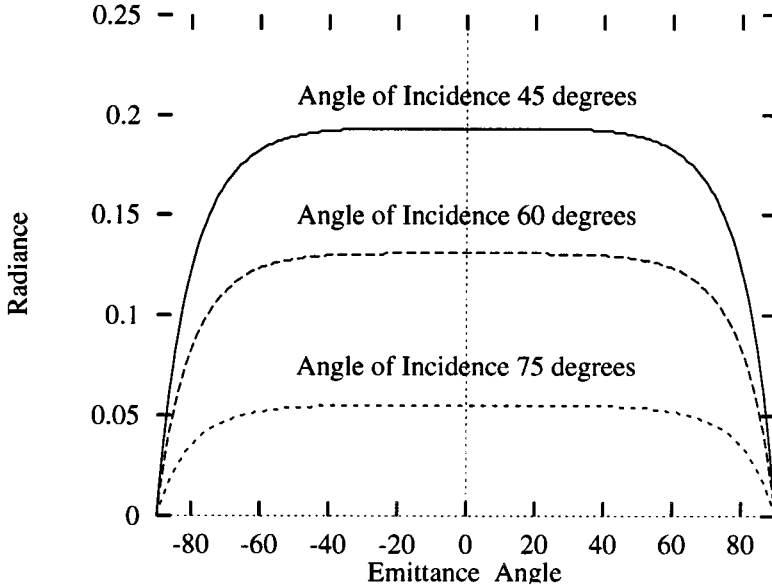


Figure 5. Prediction made by the Wolff model under the same illumination-viewing conditions as Fig. 2.

Fig. 3. Since the Wolff model does not take into account surface roughness properties the reflected diffuse radiance is symmetric with respect to angle of emittance and again is monotonically decreasing for increasing  $\theta_r$ . It is difficult to compare the Oren-Nayar model and the Wolff model under the same surface conditions since each has been clearly stated to be applicable under one of two exclusively different surface conditions, very rough and smooth respectively. So for instance, it is entirely simplistic to state that under the conditions for Fig. 3, the Oren-Nayar model predicts Lambertian diffuse reflectance depicted by the horizontal dashed line. Again, the Oren-Nayar makes the assumption of Lambertian microfacets as an approximation that is only useful under very rough surface conditions where geometry effects dominate.

There are salient qualitative differences between the behavior of diffuse reflection across rough and smooth object surfaces having significantly different normal directions across the surface (e.g., cylinder sphere, cube). Consider first the case when light is incident nearly parallel to viewing. For rough surfaces the reflected radiance of diffuse reflection will typically be *brighter* across the surface than predicted by Lambert's law. This gives rough diffuse surfaces a "flatter" appearance (e.g., the moon). On the other hand, the reflected radiance of diffuse reflection from smooth surfaces will typically be *darker* than predicted by Lambert's Law, becoming significantly less for large angles of

reflection  $\theta_r$  and/or large angles of incidence  $\theta_i$ . This gives smooth diffuse surfaces a slightly "rounder" appearance. An example of the reflected radiance distribution across an image of a cylindrical object, one with a rough surface (Fig. 6), and one with a smooth surface (Fig. 7) illustrates this significant effect.

Figures 8 and 9 show the radiance distribution across a smooth cylindrical cup for oblique incidence of a light source. Lambert's Law predicts a monotonic decreasing radiance distribution which is maximum at the occluding contour and decreasing toward the visual center of the cup. Significantly contrary to this, the smooth diffuse reflection model by Wolff, supported with empirical data, shows that reflected radiance is minimal at the occluding contour, rising to a maximum at approximately relative orientation  $65^\circ$  and then decreasing toward the visual center of the cup. According to Eq. (7), diffuse reflection from a smooth surface in the close vicinity of an occluding contour has small reflected radiance regardless of illumination geometry because  $\theta_r$  is close to  $90^\circ$ . Figure 10 shows an example of the intensity profile for diffuse reflection across a rough cylinder for a point light source incident 20 degrees relative to the viewer. It is interesting to note that for rough surfaces as the oblique incidence of light increases to 90 degrees that the intensity profile across the cylinder essentially becomes identical to that predicted by Lambertian reflectance, up to a scale factor (i.e., under very rough surface conditions the Oren-Nayar model

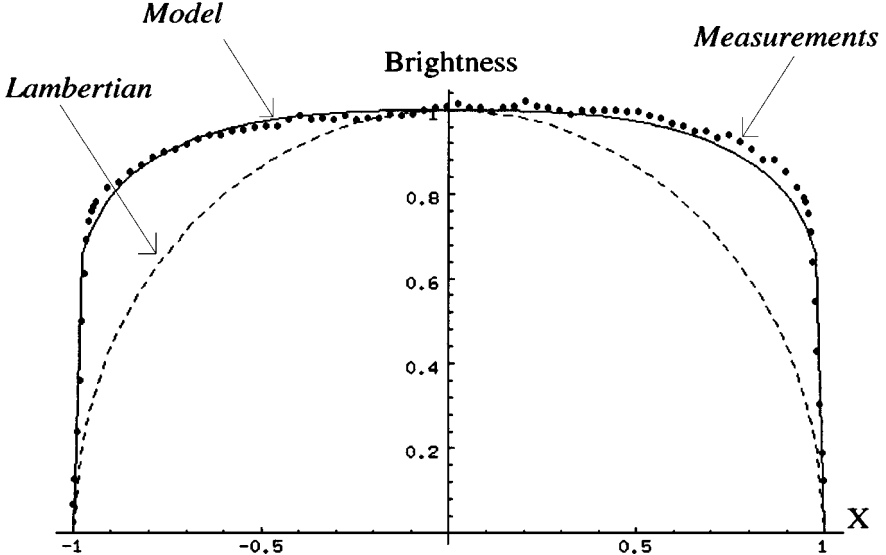


Figure 6. Image brightness across the image of a rough cylinder for  $\theta_i = 0^\circ$  (excluding specular component). Solid line is prediction by Oren-Nayar model.

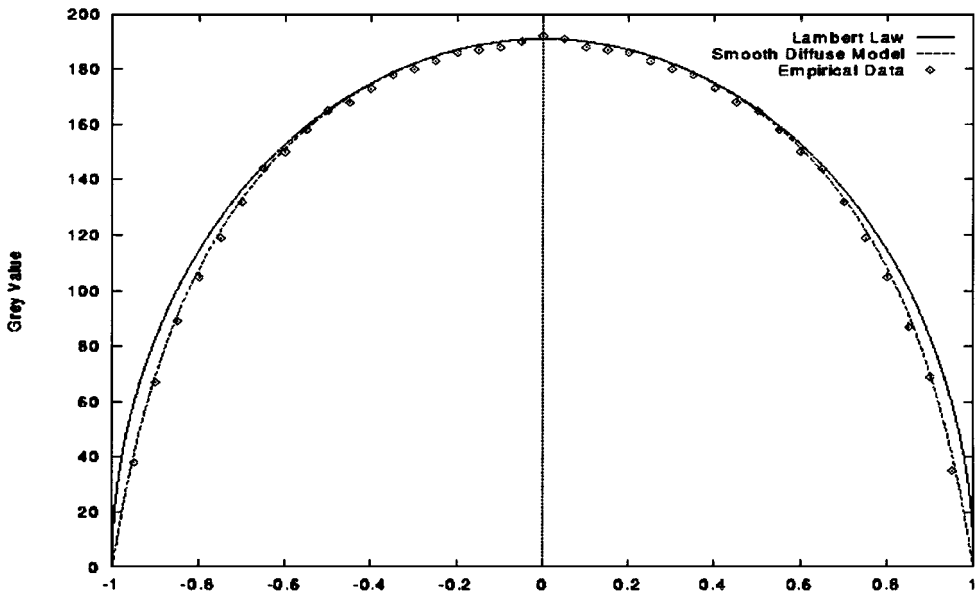


Figure 7. Image brightness across the image of a smooth cylinder for  $\theta_i = 0^\circ$  (excluding specular component). Solid line is prediction by Wolff model.

essentially predicts the dashed curves in Figs. 7 and 8, which is accurate). For Fig. 10, under smooth surface conditions, the Wolff model predicts much more agreement with the Lambert model, this Lambertian behavior significantly breaking down when the angle of incidence  $\theta_i$  exceeds  $50^\circ$ .

Interestingly, even though reflected radiance from rough surfaces has a complicated behavior with respect to illumination-viewing geometry, for near-normal light incidence (i.e., small  $\theta_i$ ) on a planar surface patch rough surfaces are more nearly “Lambertian” in terms of independence of reflected radiance with respect to

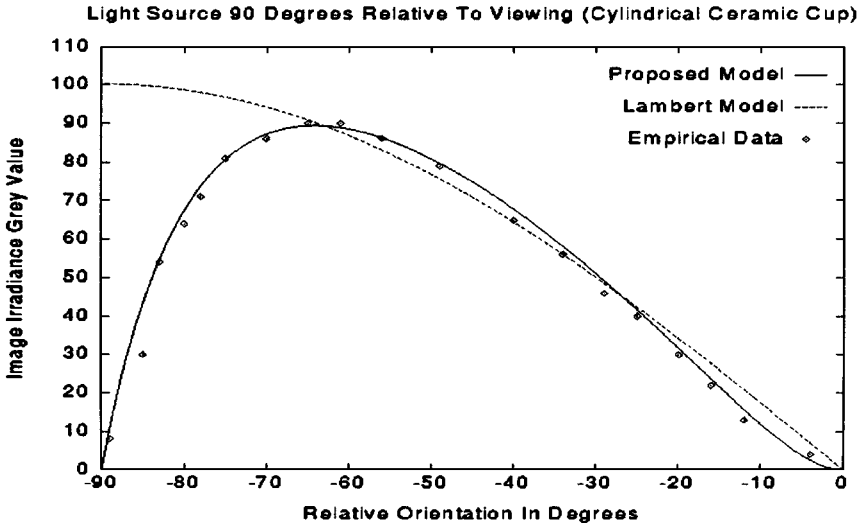


Figure 8. Diffuse reflected radiance horizontally across a smooth cylinder as a function of local surface orientation (oblique illumination  $\theta_i = 90^\circ$ ). Solid line is prediction by Wolff model.

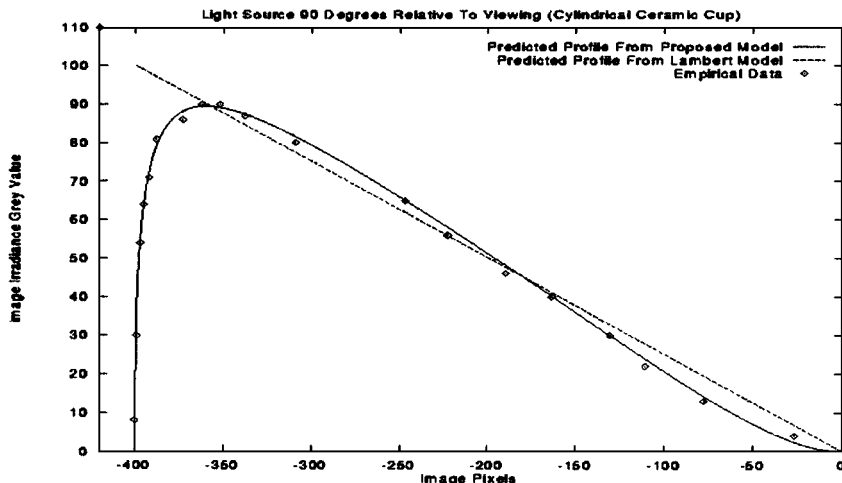


Figure 9. Same radiance across a smooth cylinder as in Fig. 7, but as a function of image pixel value. Solid line is prediction by Wolff model.

viewing direction than are smooth surfaces. Above  $\theta_i = 10^\circ$ , rough surfaces have significant viewer dependence.

For machine vision applications deciding which diffuse reflectance model is most accurate for a given surface material can use preliminary reflectance measurements respective for different  $\theta_i$  and  $\theta_r$ . As seen in Figs. 3, 4, and 5 a high degree of symmetry for reflected radiance with respect to varying  $\theta_r$  while holding  $\theta_i$  fixed at some nonzero value (i.e., direction of incidence away from the surface normal) is indicative

of a smooth surface, while asymmetry is indicative of a rough surface. The physical parameters for diffuse reflection from smooth surfaces are the index of refraction  $n$  of the surface medium and the proportional amount of conservative internal scattering  $\rho$ . Varying these parameters essentially only has the effect of scaling the amount of diffuse reflection. The roughness parameter  $\sigma$  is very important for diffuse reflection from rough surfaces, but another physical parameter can also incorporate relative scaling of  $L_r^1$  and  $L_r^2$  in Eq. (5). These two parameters can be used to empirically fit

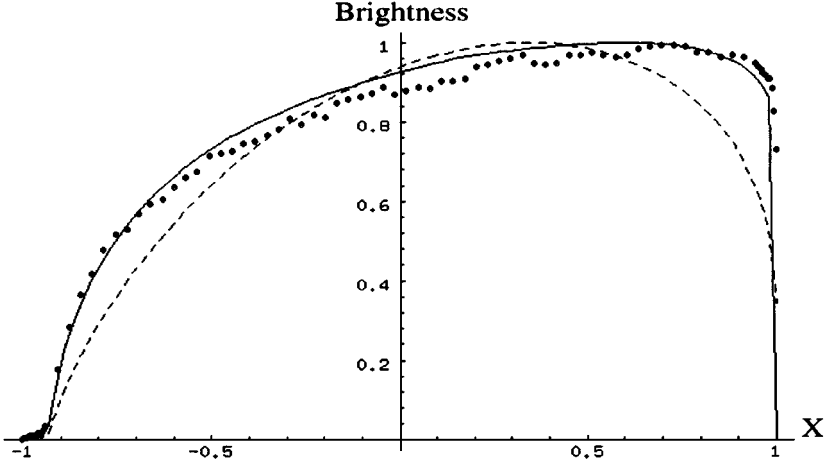


Figure 10. Image brightness across the image of a rough cylinder for  $\theta_i = 20^\circ$  (excluding specular component). Solid line is prediction by Oren-Nayar model.

the shape of measured reflectance data from rough surfaces.

### 3.2. Comparison of Visual Behavior

Figure 11(a) shows a real image of a white billiard ball illuminated by two point light sources orthogonal to viewing, one from the left side and one from the

right side. Figure 11(b) shows a computer graphics rendering of a sphere illuminated by the same configuration of two point light sources assuming Lambert's diffuse reflectance law, while Fig. 11(c) shows the same computer graphics rendering of a sphere using the smooth diffuse reflectance model (Eq. (7)). While both shadow boundaries with respect to the left and right light sources coincide along the vertically oriented great circle at the front of the sphere, there appears to be

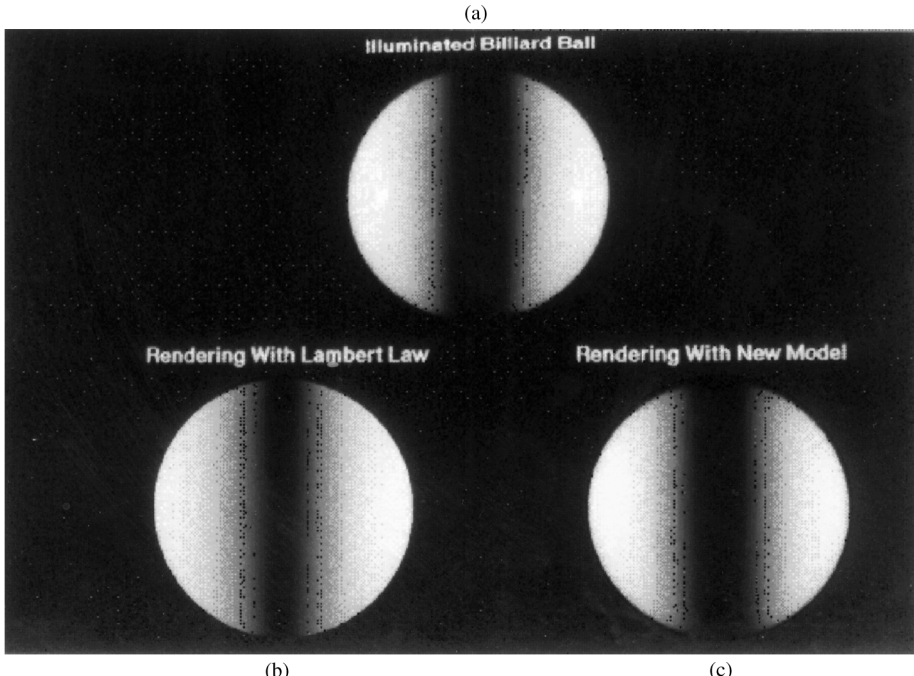


Figure 11. Intensity images of a real and rendered billiard ball. New Model means prediction by the Wolff model.

a “shadow band” of darker (i.e., smaller) intensity values about this shadow boundary due to the high fall off of diffuse reflectance at high angles of incidence near  $90^\circ$ . Observe that realistically this “shadow band” is in fact significantly wider in Fig. 11(a) than predicted by the Lambert Law in Fig. 11(b), but more accurately predicted by the proposed diffuse reflectance law in Fig. 11(c).

Figures 12(a), (b), and (c) show grey level representations of isophote curves (i.e., image curves with equal intensity) corresponding respectively to Figs. 11(a), (b), (c). Lambert’s Law predicts for this configuration of light sources illuminating a sphere that equal reflected radiance occurs for points forming concentric circles on the sphere about the left-most and right-most occluding contour points. These concentric circles of equal reflected radiance orthographically project onto straight isophote lines as depicted in Fig. 12(b), with maximum diffuse reflectance occurring at the left-most and right-most occluding contour points where the angle of incidence is zero. Any diffuse reflectance expression involving only the angle of incidence will predict the same straight geometry of isophotes. Figure 12(a) which is an actual depiction of the isophotes of Fig. 11(a) shows that, in fact, lines of equal image intensity severely curve near the occluding contour of the sphere. Maximum diffuse reflection

occurs at the center of the closed elliptical isophotes near the left-most and right-most occluding contours while diffuse reflection at the occluding contours is nearly zero, illustrating a two-dimensional version of the effect depicted in Figs. 8 and 9. Figure 12(c) shows the isophotes rendered using the smooth diffuse reflectance model (Eq. (7)) which are remarkably similar to the actual isophotes in Fig. 12(a) (except for the isophotes perturbed by the specularities). Comparing Figs. 12(a), (b), and (c) show very clearly the diffuse reflectance model for smooth surfaces accurately predicts reflectance features that are significantly deviant from Lambertian behavior.

One of the main features of the rough diffuse reflectance model is that it establishes a continuum from Lambert’s Law all the way to the linear reflectance model presented in (Horn, 1977) for lunar reflectance. Reflectance maps are widely used in vision for obtaining shape information from brightness images (Horn and Brooks, 1989). For a given reflectance model and source direction, the reflectance map establishes the relationship between surface orientation, given by the gradient space parameters  $(p, q)$ , and image brightness. Figure 13(a) shows the reflectance map of a Lambertian surface for illumination from the direction  $(\theta_i = 10^\circ, \phi_i = 45^\circ)$ . The same map is obtained using the proposed model with roughness  $\sigma = 0$ . Figure 13(b)

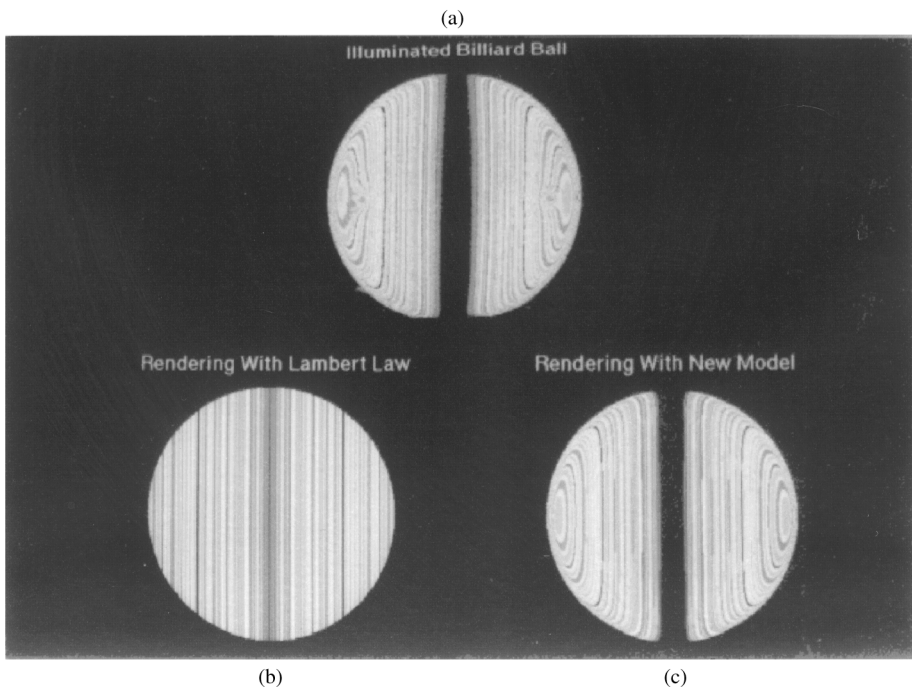


Figure 12. Isophote images of a real and rendered billiard ball. New Model means prediction by the Wolff model.

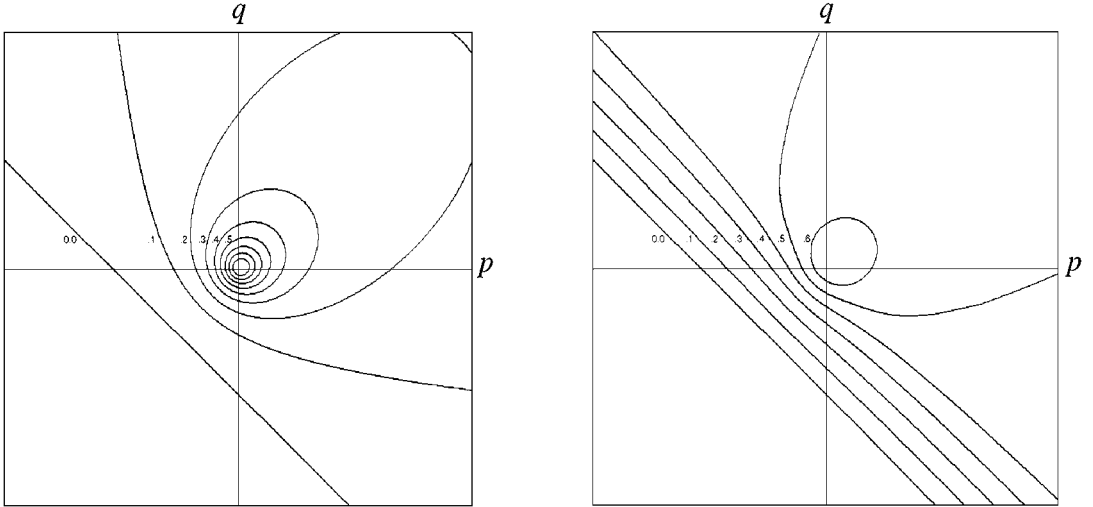


Figure 13. Reflectance maps for (Left) Lambertian surface ( $\rho = 0.9$ ), and (Right) rough diffuse surface ( $\sigma = 60^\circ$ ,  $\rho = 0.9$ ) as predicted by the Oren-Nayar model. For both maps the angles of incidence are  $\theta_i = 10^\circ$  and  $\phi_i = 45^\circ$ . Note the similarity between the second map and the well-known linear reflectance map previously suggested for lunar reflectance (see Horn and Brooks, 1989).

shows the reflectance map of a rough diffuse surface with  $\sigma = 60^\circ$ . Interestingly, the rough surface produces a map that appears very similar to the linear reflectance map (Horn and Brooks, 1989) hypothesized for the lunar surface. The proposed reflectance model therefore establishes a continuum from pure Lambertian to lunar-like reflectance. Further, the model predicts that the linearity in the reflectance map occurs only when the viewer is close to the source.

The Oren-Nayar model predicts that for very high macroscopic roughness, when the observer and the illuminant are close to one another, all surface normals will generate approximately the same brightness. This implies that, when viewing and illumination directions are similar, a three-dimensional object, irrespective of its shape, will produce nothing more than a silhouette with constant intensity within. In the case of polyhedra, edges between adjacent faces will no longer be discernible (Figs. 14(c) and (d)), and smoothly curved objects will be devoid of shading (Figs. 14(a) and (b)). This visual ambiguity may be viewed as a perceptual singularity in which interpretation of the three-dimensional shape of an object from its image is impossible for both humans and machines. This phenomenon offers a plausible explanation for the flat-disc appearance of the full moon (Fig. 14(e)). As discussed in Section 1, there have been some models developed earlier also predicting a flat appearance of the full moon (Minnaert, 1941; Hapke and van Horne, 1963).

Figure 15 shows a direct comparison of the visual appearance of a cylinder and a sphere, synthetically rendered respectively (left to right) with the Lambertian model, the Wolff model, and, the Oren-Nayar model. In support of the quantitative evidence presented in Figs. 5 and 6 in Section 3.1, compared with object surfaces obeying the Lambertian model, smooth dielectric surfaces which obey the Wolff model visually appear “rounder” while rough dielectric surfaces obeying the Oren-Nayar model visually appear “flatter”. Also note the edge of the cylinder produced from discontinuity in surface orientation; compared with the Lambertian model, this edge appears stronger for smooth surfaces obeying the Wolff model while this edge appears weaker for rough surfaces obeying the Oren-Nayar model.

#### 4. Discussion

The two diffuse reflectance models that have been compared are complementary in their respective applicability to surfaces with different roughness conditions. The diffuse reflection model for rough surfaces has the limitation that as roughness  $\sigma \rightarrow 0$ , diffuse reflectance is predicted to become Lambertian, a phenomenon that is not supported by the diffuse reflection model for smooth surfaces and corresponding empirical evidence. On the other hand, the diffuse reflection model

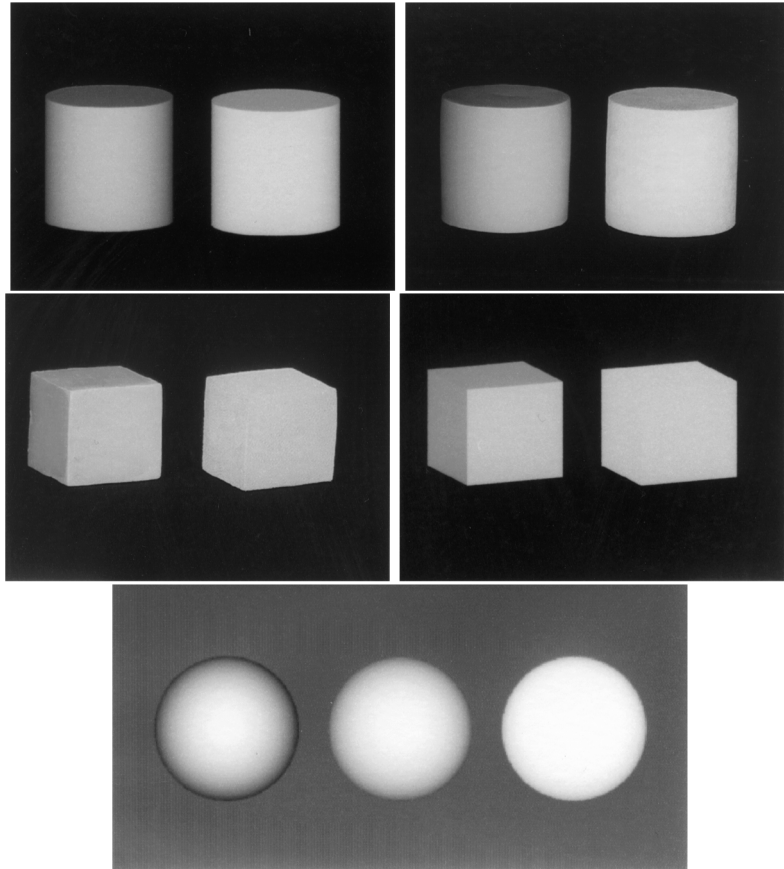


**Figure 14.** (Adopted from (Nayar and Oren, 1995)) (a) Top-Left: Camera image of two cylinders made from exactly the same material (porcelain) and illuminated from approximately  $10^\circ$  above the camera. The right vase is much rougher than the left one resulting in flatter appearance. (b) Top-Right: Synthetic image of cylinders with similar dimensions, rendered using the theoretical model (left:  $\sigma = 5^\circ$ , right:  $\sigma = 35^\circ$ ). (c) Middle-Left: Camera image of two cubes made from stoneware, illuminated from approximately  $18^\circ$  to the left of the camera. (d) Middle-Right: Synthetic image of cubes (left:  $\sigma = 7^\circ$ , right:  $\sigma = 40^\circ$ ). In both real and synthetic images, low macroscopic roughness of the left cube results in nearly Lambertian appearance, whereas very high roughness of the right cube causes all three faces to produce almost the same brightness with clear edges no longer visible. The model and experiments suggest that for very high macroscopic roughness, when source and sensor directions are close to one another, all surface normals generate the same image brightness. Alternately, any object, irrespective of its three-dimensional shape, produces just a silhouette making it impossible to perceive shape. (e) Bottom: Spheres illuminated and viewed from the same direction. As roughness increases (left to right:  $\sigma = 0^\circ$ ;  $\sigma = 15^\circ$ ;  $\sigma = 40^\circ$ ) shading becomes flatter. For extreme roughness (right), the sphere appears like a flat disc, as observed in the case of the full moon.

for smooth surfaces is limited to smooth surfaces only up to a certain level of surface roughness. Two important questions to ask are:

- Below what level of roughness  $\sigma$  does the smooth diffuse reflectance model become accurate?
- Above what level of roughness  $\sigma$  does the rough diffuse reflectance model begin to become accurate?

One way to begin answering these questions is to combine the methodologies used in each of the

respective diffuse reflectance models. Accurate prediction of diffuse reflection from rough surfaces fundamentally relies upon description of local surface geometry (i.e., V-groove microfacets) together with an assumption of reflectance for each microfacet (e.g., Lambertian reflectance). Accurate prediction of diffuse reflection from smooth surfaces fundamentally relies upon description of subsurface optical scattering and air-dielectric boundary conditions. As  $\sigma \rightarrow 0$  the diffuse reflectance model for rough surfaces becomes Lambertian because of the assumption that microfacets

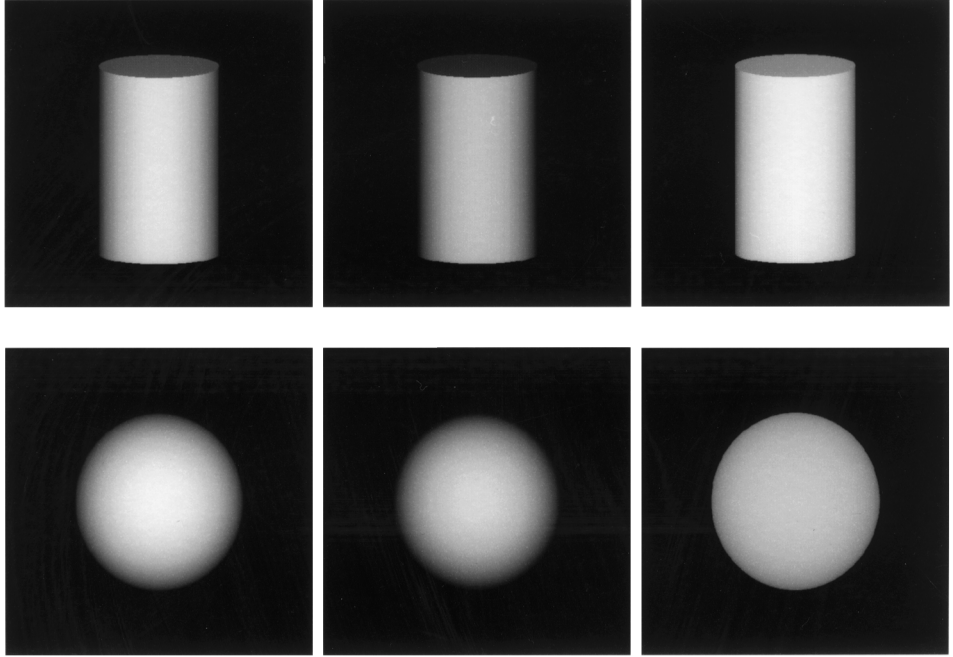


Figure 15. Synthetically rendered cylinder and sphere which from left to right respectively uses the Lambertian Model, the Wolff model, and, the Oren-Nayar Model ( $\sigma = 70^\circ$  for the rough cylinder, and,  $\sigma = 40^\circ$  for the rough sphere).

themselves are inherently Lambertian. Consider then simultaneously combining the two methodologies by making the assumption that each microfacet reflects according to the smooth diffuse reflectance model Eq. (7). Incorporating the methodology of Wolff into the methodology of Oren and Nayar formally requires the evaluation of some complicated integrals, but a simple approximation of a diffuse reflectance model that accounts for the observed empirical data presented above for both rough and smooth dielectrics can be obtained by setting in Eq. (3):

$$C_1 = \left( 1 - 0.5 \frac{\sigma^2}{\sigma^2 + 0.33} \right) \times (1 - F(\theta_i, n)) \\ \times \left( 1 - F\left(\sin^{-1}\left(\frac{\sin \theta_r}{n}\right), 1/n\right) \right) \quad (9)$$

for the appropriate range of  $\sigma$ . Neglecting interreflections, for the rough diffuse reflectance model described by Eq. (3) as currently written, the Lambertian term dominates when

$$\left( 1 - 0.5 \frac{\sigma^2}{\sigma^2 + 0.33} \right) \gg 0.45 \frac{\sigma^2}{\sigma^2 + 0.09}$$

The tan functions in Eq. (3) that are multiplied by  $C_2$  and  $C_3$  only become significant in value when both  $\theta_i$  and  $\theta_r$  are simultaneously above  $80^\circ$ . The term  $C_1$  is at least a factor of 10 greater than both  $C_2$  and  $C_3$  for surface roughness,  $\sigma < 9^\circ$ , at least a factor of 20 for  $\sigma < 6^\circ$ , and at least a factor of 100 for  $\sigma < 2.5^\circ$ . Hence, an approximate answer to the first question above is that the smooth diffuse reflectance model becomes applicable for a Gaussian Slope Roughness standard deviation  $\sigma$  in this range for which the term  $C_1$  in expression (9) should be used in Eq. (3).

There is an intermediate range of surface roughness values  $\sigma$  where both local surface geometry effects of masking, shadowing, and possibly interreflection contribute as much as accounting for reflectance from each microfacet from subsurface scattering and air-dielectric boundary modeling. It is in this intermediate roughness “transition range” that a reflectance model combining the rough diffuse reflectance model with an assumption of microfacet reflectance based upon the smooth diffuse reflection model, may be more accurate. A simplified qualitative answer to the second question above can be obtained by asking what values of surface roughness  $\sigma$  is the value of  $0.45 \frac{\sigma^2}{\sigma^2 + 0.09}$  comparable in size to  $C_1$ ? The graph in Fig. 16 shows the values of these terms for

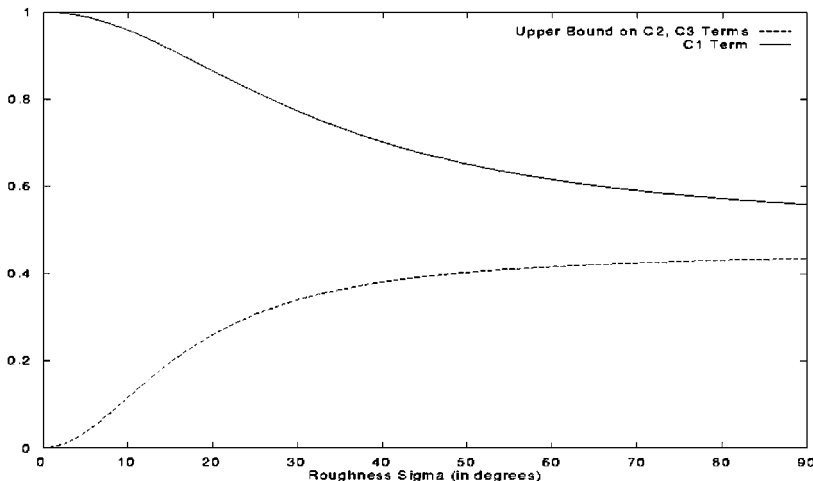


Figure 16. Graphed values of  $C_1$  (Eq. (9)) and upper bound for  $C_2, C_3$  coefficients (from the original Eq. (3)) for diffuse reflectance model against surface roughness  $\sigma$ .

different  $\sigma$ . The value of  $0.45 \frac{\sigma^2}{\sigma^2 + 0.09}$  is at least  $1/2$ ,  $1/3$ , and  $1/4$  of  $C_1$  for roughness values  $\sigma$  greater than  $36^\circ$ ,  $22^\circ$ , and  $17^\circ$ , respectively. The upper bound  $\sigma$  for the intermediate transition range probably lies somewhere between these values.

Even though it is clear that in general the Lambertian Model is not always accurate in describing diffuse reflection from both rough and smooth surfaces, because of the simplicity of such a model it is still of great importance for computer vision researchers to know under what physical conditions Lambert's Law can be applied to good approximation. This may elegantly simplify some vision algorithms under some important circumstances. For instance for smooth surfaces, the Lambertian model is accurate within a margin of about 5% when  $\theta_r$  and  $\theta_i$  are simultaneously less than  $50^\circ$ .

## 5. Summary and Conclusion

Two recently developed diffuse reflectance models have been presented and compared for rough and smooth dielectric surfaces. Together these models accurately predict both quantitative and visual diffuse reflection effects for smooth dielectric surfaces and very rough dielectric surfaces. These diffuse reflectance models fill a significant gap that has existed in the computer vision literature for methodologies that are dependent upon diffuse reflected photometric values. Lambert's Law is commonly used in such methodologies as shape from shading, and the

presented diffuse reflectance models can be used to explain the conditions under which Lambert's Law is most accurate. Limitations of both these diffuse reflectance models were explained. Diffuse reflection from surfaces with 'intermediate' roughness exhibit a combination of effects produced both from internal scattering and external roughness conditions that is not yet accurately explained. A methodology for how these two models can be combined was presented suggesting one possible direction for explaining diffuse reflection over a broader physical range of roughness conditions.

## Notes

1. A different backscattering mechanism, called retroreflection or opposition effect, produces a sharp peak close to the source direction (see Hapke and van Horne, 1963; Kuga and Ishimaru, 1984; Tsang and Ishimaru, 1984; Oetking, 1966). A recent article by Hapke et al. (1993) throws new light on this mechanism. It is seldom encountered in machine vision since it is observed only when the sensor and source are within a few degrees from each other; a situation difficult to emulate in practice without the source or the sensor occluding the other.
2. The *plane of incidence* is defined by the incident and surface normal directions.

## References

- Bahar, E. 1987. Review of the full wave solutions for rough surface scattering and depolarization. *Journal of Geophysical Research*, 92(C5):5209–5224.  
 Beckmann, P. and Spizzichino, A. 1963. *The Scattering of Electromagnetic Waves from Rough Surfaces*. Macmillan.

- Buhl, D., Welch, W.J., and Rea, D.G. 1968. Reradiation and thermal emission from illuminated craters on the lunar surface. *Journal of Geophysical Research*, 73(16):5281–5295.
- Cabral, B., Max, N., and Springmeyer, R. 1987. Bidirectional reflection functions from surface bump maps. *ACM Computer Graphics (SIGGRAPH 87)*, 21(4):273–281.
- Chandrasekhar, S. 1960. *Radiative Transfer*. Dover Publications: New York.
- Fresnel, A.J. 1866. Memoire sur la reflexion de la lumiere polarisee. *The Complete Works of Fresnel*, 1:767–775 (published posthumously).
- Gondek, J.S., Meyer, G.W., and Newman, J.G. 1994. Wavelength dependent reflectance functions. *Computer Graphics Proceedings (SIGGRAPH 94)*, pp. 213–220.
- Grimson, W.E.L. 1984. Binocular shading and visual surface reconstruction. *Computer Vision Graphics and Image Processing*, 28(1):19–43.
- Hanrahan, P. and Krueger, W. 1993. Reflection from layered surfaces due to subsurface scattering. *Computer Graphics Proceedings (SIGGRAPH 93)*, pp. 165–174.
- Hapke, B.W. and van Horne, H. 1963. Photometric studies of complex surfaces, with applications to the moon. *Journal of Geophysical Research*, 68(15):4545–4570.
- Hapke, B.W., Nelson, R.M., and Smythe, W.D. 1993. The opposition effect of the moon: The contribution of coherent backscatter. *Science*, 260(23):509–511.
- Healey, G. 1989. Using color for geometry-insensitive segmentation. *Journal of the Optical Society of America A*, 6(6):920–937.
- Hering, R.G. and Smith, T.F. 1970. Apparent radiation properties of a rough surface. *AIAA Progress in Astronautics and Aeronautics*, 23:337–361.
- Horn, B.K.P. 1977. Understanding image intensities. *Artificial Intelligence*, 8(2):201–231.
- Horn, B.K.P. and Brooks, M.J. 1989. *Shape From Shading*. MIT Press.
- Kajiya, J.T. 1991. Anisotropic reflection model. *ACM Computer Graphics (SIGGRAPH 91)*, 25(4):175–186.
- Kubelka, P. and Munk, F. 1931. Ein Beitrag sur optik der farbanstriche. *Z. Tech.*, 12:593.
- Kuga, Y. and Ishimaru, A. 1984. Retroreflectance from a dense distribution of spherical particles. *Journal of the Optical Society of America A*, 1(8):831–835.
- Lambert, J.H. 1760. *Photometria Sive de Mensura de gratibus lumenis, colorum et umbrae*. Eberhard Klett: Augsberg, Germany.
- Minnaert, M. 1941. The reciprocity principle in lunar photometry. *Astrophysical Journal*, 93:403–410.
- Nayar, S.K., Ikeuchi, K., and Kanade, T. 1991. Surface reflection: Physical and geometrical perspectives. *IEEE Transactions on Pattern Analysis and Machine Intelligence*, 13(7):611–634.
- Nayar, S.K. and Oren, M. 1995. Visual appearance of matte surfaces. *Science*, 267:1153–1156.
- Nicodemus, F.E., Richmond, J.C., Hsia, J.J., Ginsburg, I.W., and Limperis, T. 1977. Geometrical considerations and nomenclature for reflectance. National Bureau of Standards, NBS monograph 160.
- Oetking, P. 1966. Photometric studies of diffusely reflecting surfaces with application to the brightness of the moon. *Journal of Geophysical Research*, 71(10):2505–2513.
- Opik, E. 1924. Photometric measures of the moon and the moon the earth-shine. *Publications de L'Observatoire Astronomical de L'Universite de Tartu*, 26(1):1–68.
- Orchard, S. 1969. Reflection and transmission of light by diffusing suspensions. *Journal of the Optical Society of America*, 59(12):1584–1597.
- Oren, M. and Nayar, S. 1992. Diffuse reflection model for rough surfaces. Columbia University Technical Report CUCS-057-92.
- Oren, M. and Nayar, S. 1993a. Generalizing Lambert's law. In *Proceedings of the DARPA Image Understanding Workshop*, Washington, DC, pp. 1025–1030.
- Oren, M. and Nayar, S. 1993b. Diffuse reflectance from rough surfaces. In *Proceedings of the IEEE Conference on Computer Vision and Pattern Recognition (CVPR)*, New York.
- Oren, M. and Nayar, S.K. 1994. Seeing beyond Lambert's law. In *Proceedings of the Fourth European Conference on Computer Vision (ECCV)*, Stockholm, pp. 269–280.
- Oren, M. and Nayar, S.K. 1995. Generalization of the Lambertian model and implications for machine vision. *International Journal of Computer Vision*, 14(3):227–251.
- Orlova, N.S. 1956. Photometric relief of the lunar surface. *Astron. Z.*, 33(1):93–100.
- Poulin, P. and Fournier, A. 1990. A model for anisotropic reflection. *ACM Computer Graphics (SIGGRAPH 90)*, 24(4):273–282.
- Reichman, J. 1973. Determination of absorption and scattering coefficients for nonhomogeneous media 1: Theory. *Applied Optics*, 12(8):1811–1815.
- Siegel, R. and Howell, J.R. 1981. *Thermal Radiation Heat Transfer*. McGraw-Hill.
- Smith, B.G. 1967. Lunar surface roughness: Shadowing and thermal emission. *Journal of Geophysical Research*, 72(16):4059–4067.
- Smith, G.B. 1986. Stereo integral equation. In *Proceedings of the AAAI*, pp. 689–694.
- Torrance, K. and Sparrow, E. 1967. Theory for off-specular reflection from roughened surfaces. *Journal of the Optical Society of America*, 57:1105–1114.
- Tsang, L. and Ishimaru, A. 1984. Backscattering enhancement of random discrete scatterers. *Journal of the Optical Society of America A*, 1(8):836–839.
- Westin, H.W., Arvo, J.R., and Torrance, K.E. 1992. Predicting reflectance functions from complex surfaces. *ACM Computer Graphics (SIGGRAPH 92)*, 26(2):255–264.
- Wolff, L.B. 1991. On diffuse reflection. Johns Hopkins Technical Report CS-91-18.
- Wolff, L.B. 1992a. A diffuse reflectance model for dielectric surfaces. In *Proceedings of the SPIE Conference on Optics, Illumination, and Image Sensing for Machine Vision VII*, Boston, MA, vol. 1822, pp. 60–73.
- Wolff, L.B. 1992b. Diffuse reflection. In *Proceedings of IEEE Conference on Computer Vision and Pattern Recognition (CVPR)*, Urbana-Champaign Illinois, pp. 472–478.
- Wolff, L.B. 1993a. Diffuse reflection from smooth dielectric surfaces. In *SPIE Proceedings of Optical Scattering: Applications, Measurement, and Theory II*, San Diego, CA, SPIE, pp. 26–44.
- Wolff, L.B. 1993b. Specular and diffuse reflection. In *Proceedings of the DARPA Image Understanding Workshop*, Washington, DC, pp. 1031–1037.
- Wolff, L.B. 1994a. A diffuse reflectance model for smooth dielectrics. *Journal of the Optical Society of America (JOSA)* (special issue on Physics Based Machine Vision), 11(11):2956–2968.
- Wolff, L.B. 1994b. Relative brightness of specular and diffuse reflection. *Optical Engineering*, 33(1):285–293.